

Modeling and process planning for curved layer fused deposition

Yuan Jin¹ · Jianke Du¹ · Yong He² · Guoqiang Fu³

Received: 22 July 2016 / Accepted: 7 November 2016 / Published online: 18 November 2016
© Springer-Verlag London 2016

Abstract Fused deposition modeling (FDM), one of the earliest and typical additive manufacturing (AM) technologies, holds great potential in a wide range of industrial applications due to their increasing availability, simplicity, affordability, and capability to fabricate both prototypes and functional parts without limitation on geometric complexity. Notwithstanding many evident advantages over traditional subtractive manufacturing methods, there are still some limitations of this rapidly developing technique. One intractable problem is the undesirable surface finish from the layer-by-layer manufacturing process, where the stair-step issue appears unavoidably. This problematic phenomenon becomes much more serious when fabricating the surface with some minute but critical features. In order to solve these problems, curved layer manufacturing method is a good substitute for general flat fused deposition modeling. This work is an exploratory study for curved layer fused deposition (CLFD), involving the modeling and process planning, which are the foundation for the implementation of CLFD. The physical model for CLFD is developed firstly, and subsequently, the process planning, including the slicing procedure and the extruder path generation, is analyzed and presented. The output from the process planning could be applied in the fabrication of curved surfaces, which would possess tiny features and exhibit excellent

smoothness instead of annoying exterior appearance. At last, the implementation of the proposed strategies and approaches on a bowl-like surface is provided to verify the effectiveness and advantages of CLFD.

Keywords Additive manufacturing · Curved layer fused deposition · Slicing procedure · Path planning

1 Introduction

Additive manufacturing, also termed as rapid prototyping in its early stage, and less formally as 3D printing, refers to a group of layer-based joining processes that builds physical shapes and structures directly from virtual models [1]. These fabrication techniques are characterized by successive deposition of semi-solid, powder-based or liquid-based materials within a certain area on each layer to form a solid section of the part, thus fundamentally different from conventional subtractive manufacturing techniques [2]. Among different AM technologies, FDM is the most widely used because of its easy accessibility and long-term development [3]. FDM is a filament extrusion-based process, where the semi-molten thermoplastic filament is extruded from a heated nozzle onto the platform and deposited line by line to form a two-dimensional layer driven by the motion control system accurately. The semi-molten material on the plate solidifies quickly since the atmospheric temperature is much lower than the polymer melting point. In the fabrication process, the deposition lines are expected to be integrated into its adjacent lines both horizontally by controlling the gap between lines and vertically via its own gravity and the force from the extruder [4].

Although the layer-based FDM process can realize the fabrication of any parts with complex internal structures, there are some shortcomings and drawbacks coming with its

✉ Yuan Jin
jinyuan@nbu.edu.cn

¹ School of Mechanical Engineering and Mechanics, Ningbo University, Ningbo 315211, China

² School of Mechanical Engineering, Zhejiang University, Hangzhou 310027, China

³ School of Mechanical Engineering, Southwest Jiaotong University, Chengdu 610031, China

advantages, like the poor geometrical accuracy and undesirable surface finishing [5]. The fundamental reasons behind these problems include stair-step effect on the side surface of the part, the rounding of sharp corners, the shape of extruded filaments, air gaps between adjacent lines, and so on [6]. At the same time, the mentioned weaknesses can be explained from the perspective of process planning stage: the original design model is converted to STL file format firstly, which uses large number of triangles to represent to the boundary of solid parts. Besides, the slicing procedure utilizes large number of slices to represent the virtual model. These two approximations of the surface geometry bring in the difference between the virtual design model and the practical fabrication solid model. In the extrusion and deposition process, the extruded filament cannot cover the planned path fully near sharp corners, which means some gaps and overlaps would appear in this case.

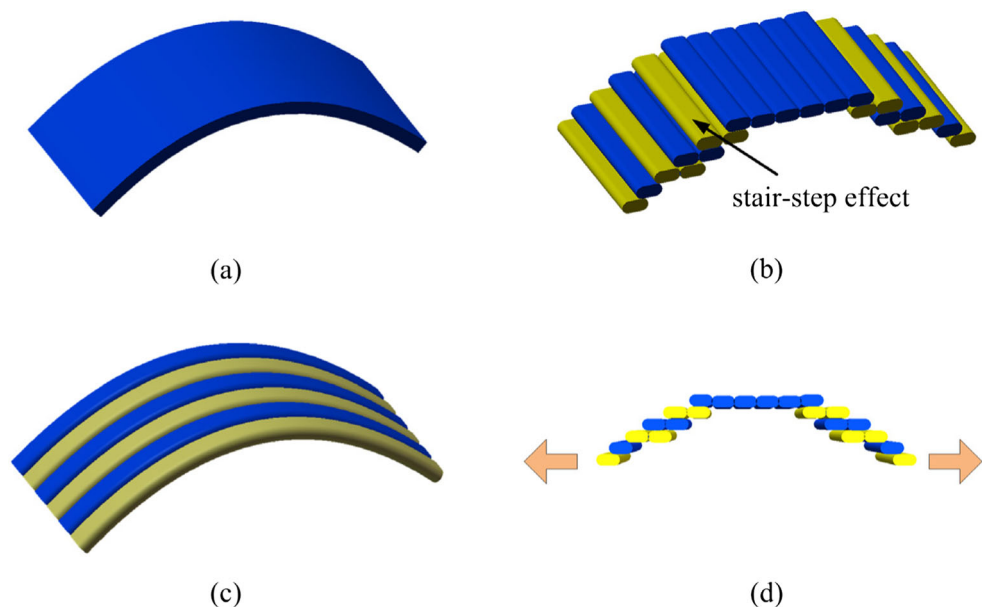
The occurrence of aforementioned issues would definitely affect the regular use and functionality of fabricated parts, especially for those which have high accuracy requirement, and is difficult to predict and compensate [7]. Much research has been dedicated to model the surface profile of fabricated objects in the FDM process [3, 8–10]. Based on the developed surface profile model, various approaches to improving the surface quality have been proposed [5, 11–17]. Although some of these approaches did bring in certain improvements of the surface quality, there were still some shortcomings difficult to solve. For example, the stair-step effect is impossible to completely avoid from the process planning stage, and even if the post-processing can, to some extent, relieve the roughness of the stripy surface, the geometric accuracy is not easy to guarantee during this process as the post-processing parameters are very hard to control accurately. Additionally, the

bonding strength between adjacent layers has been long criticized when the contact area between layers is relatively small. It is not easy to find a good solution to this problem except by increasing the force when stacking the material, but this will lead to some deformation that is not good for the modeling accuracy.

Aiming at addressing those problems that are not easy to solve in general flat layer manufacturing methods, a potential and feasible method is curved layer fused deposition (CLFD), where the filaments are deposited along curved (essentially non-horizontal) paths instead of planar paths [18]. This novel building paradigm for FDM would result in better material structure and part strength because of the fiber continuity along the extrusion path. In addition, the fabrication of curved surface with small curvature variation in Fig. 1a is very difficult to achieve accurate and smooth surface using conventional flat fused deposition due to the serious stair-step effect as shown in Fig. 1b. In contrast, it is easy and convenient for CLFD to fabricate the smooth surface without stair-step issue as shown in Fig. 1c. Besides, the shell-like part would achieve a much better mechanical strength using CLFD instead of flat FDM as shown in Fig. 1d. Overall, it is believable that there are some types of shapes or structures that can achieve considerable improvements in part performance or convenience in the fabrication with the implementation of CLFD [19].

Chakraborty et al. [18] proposed the definition of curved layer FDM firstly by investigating the manufacturing of curved thin parts with the proposed method and found that there would be substantial improvements in the mechanical properties of fabricated parts compared to general FDM process. Specifically, they studied the extruder path generation for CLFD with two identified criteria: proper orientation of filaments and appropriate bonding between adjacent filaments

Fig. 1 Construction of fabricated part with curved layer and general flat fused deposition. **a** 3D model for fused deposition modeling. **b** Fabricated model with flat FDM. **c** Fabricated model with CLFD. **d** Demonstration of bad mechanical strength



in the same layer and in the successive layers. In the determination of the filament orientations and interval, the cross section of the deposited filament was approximated with circles to make it similar to the traditional CNC path planning for referring related methods and algorithms. Although this approximation could reduce the complexity for the path planning in CLFD, some of key factors in the path planning for CLFD would be neglected on the basis of this assumption. For example, the optimal distances between adjacent filaments in the same layer and in the successive layers are uniform when the cross section of the filament is assumed as circular, but it is not true in the practical deposition process. So, the geometry of the deposited filaments should be considered with a more accurate way.

In addition, Huang and Singamneni [20, 21] developed an AM machine that could additively fabricate models with curved layers that represented the natural shape of parts. With this hardware, they contributed to developing some necessary and important algorithms for the process planning in CLFD, including modeling and evaluation [22], slicing and deposition strategies [23, 24], as well as combination of CLFD and flat FDM [25, 26]. Their works laid a solid foundation for the development and diffusion of CLFD. However, many critical details and technical methods were not provided. For example, they tried to study some basic schemes for the curved layer fabrication, including the data generation, curved slicing, and support generation, but they just formulated some key issues of the curved surface offsetting process [22]. As for the extruder path generation, they directly adopted the output G and M code data generated by the manufacturing module in UGNX (a popular CAM software) and transferred to deposition pathways for curved layer FDM. This practice would definitely neglect some important characteristics of AM and the optimization of path planning could not be implemented. Therefore, further studies in the process planning of CLFD are required, especially in the curved slicing and extruder path planning.

Besides, Patel et al. [19] adopted the CLFD to fabricate models having randomly located, small-dimensioned but critical surface features and proposed a curved layer slicing method to capture minute critical features with the minimum number of layers achieved by mathematical method. They mainly focused on effectively capturing minute critical features of parts with the minimum number of layers by clustering the critical points and fitting these critical points into spline surfaces. However, the definition of curved slicing in this study was fundamentally different from general curved slicing and the application of the proposed algorithms was restricted seriously.

Allen et al. [27] conducted an interesting experimental investigation of CLFD utilizing a delta style deposition system, focusing on the generation of the tool path. For the curved layer path generation, they proposed a simple mathematical

approach specifically for their experimental study. The path was generated by converting the surface to an array of data points in the x - y plane over a grid of equal size at first and creating a vector field that follows the data points sequentially. The obtained vector field was then converted to an appropriate path file considering dynamic z movements and extrusion values calculated from individual vector magnitudes. However, this simple path generation method did not take any factors on deposition quality into account, and the path orientations were limited to 0° and 90° within the plane of the surface; this fact would restrict its availability and applicability.

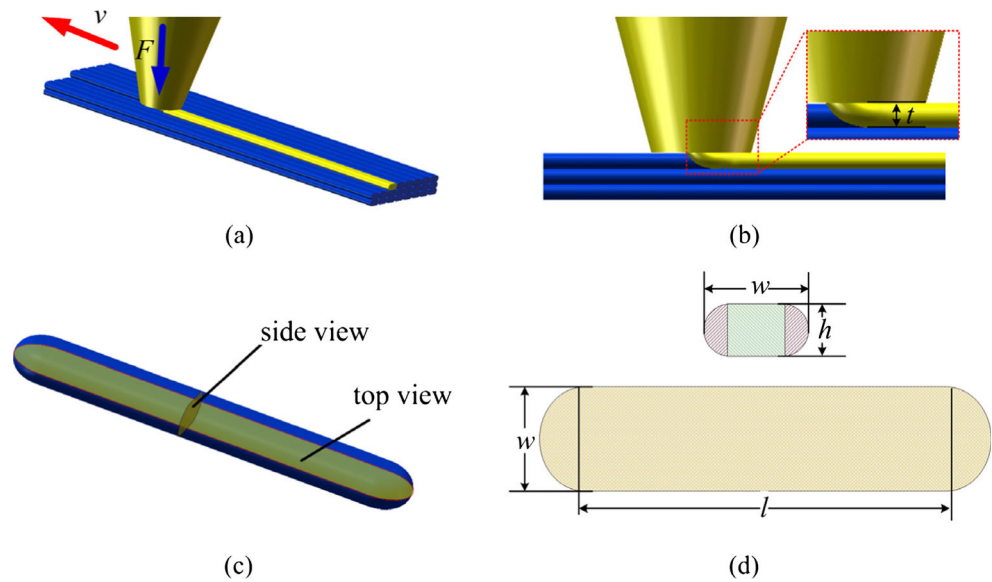
Unlike the general flat FDM that has been well studied and developed for decades and has reached an acceptable level in many aspects, CLFD still needs to be further studied in terms of modeling and process planning, especially in the extruder path generation that largely differs from that in the flat fused deposition. Indeed, some initial studies on the process planning of CLFD have been conducted. However, to the best of our knowledge, few researchers have attempted to study the major differences of CLFD and general FDM from the perspective of process planning. Moreover, the detailed methods and algorithms for the process planning that are very important in the practical implementation are still lacking as well. Therefore, this paper primarily focuses on the development of a comparatively accurate model for CLFD based on the practical filament model under deposition condition. After that, some critical algorithms for the process planning are described based on the model for the implementation of CLFD.

The remainder of this paper is constructed as follows: In Section 2, the model of CLFD is developed to investigate and analyze its process planning with some basic studies of general flat deposition modeling. Section 3 describes some algorithms for the process planning based on the established model, including the slicing strategy and the extruder path generation. Section 4 gives an example of the implementation of the proposed methods and algorithms on a bowl-like surface for evaluation, together with some discussions. Finally, a conclusion is drawn in Section 5.

2 Modeling of curved layer fused deposition

In the general flat FDM, the cross-sectional shape of the filament is primarily determined by the mechanical interaction between the nozzle tip and the base plate (or the former deposited part). The initial cross-sectional shape of the extruded filament is circle defined by the shape of the nozzle tip, and some transformation occurs when the molten polymer is landed on the base plate (or the former deposited part). As shown in Fig. 2, the cross-sectional shape of the deposited filament may be described as the drum-like shape and can be approximated with two semi-circles and a rectangle based on large

Fig. 2 Modeling of extrusion and deposition process in FDM. **a** Modeling of fused deposition process. **b** Side view of (a). **c** The shape of deposited filament. **d** The geometric detail of the filament



numbers of experiments as discussed in our former work [10]. Two critical parameters of the deposited filament's dimension are the height h and the width w , which are determined by the layer thickness t set in the slicing stage and the proportional relation between the moving velocity of the nozzle v and the flowrate of molten polymer F .

The above geometric model can be adopted to simulate the flat FDM process, including both the part surface profile and the inner geometric structures, and to analyze the mechanical performance based on the geometric distribution. In the construction of the geometric profile, the interaction between deposition filaments on one layer (between lines) and between layers should be both taken into account. In other words, the surface profile is determined by the bonding effect between adjacent deposited filaments within one layer and the joining effect between filaments on adjacent layers. However, it is not the case in the CLFD.

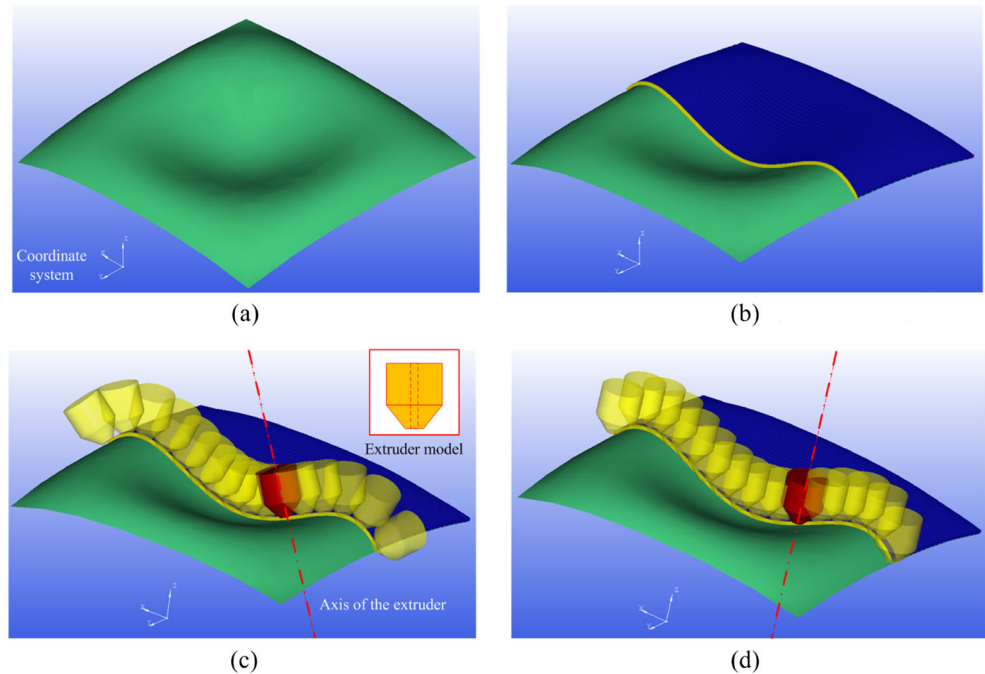
In the CLFD, the normal vectors of the surface at deposition points along a continuous path are always changing; the ideal strategy is to ensure that the extruder axis is perpendicular to the surface all the time, so that the extruded filament can be deposited accurately and joined to the former layers by applying vertical force from the extruder tip. As shown in Fig. 3c, the extruder orientation is adjusted simultaneously when the nozzle moves along the path. In order to achieve this goal, a 5-axis platform is required to change the relative orientation between the extruder and part surface. Under this circumstance, some advantages of additive manufacturing, such as economy and simplicity of system control, do not exist, which is contrary to the original intention of additive manufacturing. Fortunately, a common 3-axis FDM machine would satisfy the requirements for the fabrication of curved surface whose normal vectors do not deviate from the building direction largely. In this case, the extruder orientation keeps

uniform and coincides with the building direction (commonly bottom up) no matter how the surface normal changes, as displayed in Fig. 3d. The CLFD discussed in this paper is the latter with the assumption that the part surface to be fabricated is slightly curved that is not easy to achieve desirable surface finish and mechanical strength in flat FDM. This assumption is based on the fact that the stair-step effect on the surface whose normal deviate from the vertical direction much more largely is much less appreciable.

In the flat FDM, the extruded filament is deposited and shaped by the nozzle tip as illustrated in Fig. 2b; the nozzle tip's edge is in contact with the top surface of the extruded filament and the distance between the nozzle tip and former layers should be equal to the layer thickness t . Besides, the height of the deposited filament's cross section h is the layer thickness theoretically. However, it is not the same in the case of CLFD. As shown in Fig. 4b, the distance between the nozzle tip and former layer should be slightly larger than the thickness of the deposited filament t ; otherwise, the edge of nozzle tip may deteriorate the top surface of shaped filaments since the fabricating surface is curved. Based on this, the cross section of deposited filament differs from that in flat FDM as shown in Fig. 4c–d. In other words, the filament extruded from the nozzle tip is not shaped by the tip's edge but changes itself due to the spreading behavior during the extrusion and deposition process [28]. Therefore, the final shape of the deposited filament in CLFD can be described as oval, whose geometric parameters are affected by the material property, the polymer extrusion dynamics and so on, which is beyond the scope of this paper.

To reproduce the part surface as well as strengthen the bonds between filaments, the overlap between neighboring filaments should be kept with a proper value. Specifically, just like the case of flat FDM, the distance

Fig. 3 Extruder location along a path on the curved surface with adjusted and uniform orientation. **a** Curved surface to be fabricated. **b** Deposited paths on the surface. **c** Adjusted extruder orientation along the normal direction of points on the path. **d** Uniform extruder orientation along vertical direction



between lateral filaments is supposed to be a constant and proper value to guarantee sufficient contact between adjacent filaments, hence achieve uniform and enough bonding strength along the direction that is perpendicular to the path. Obviously, it is much more difficult to ensure that adjacent extruder paths would have uniform interval on the curved surface in CLFD compared to the flat FDM, where all deposited filaments within one layer lie on the same plane. At the same time, the bonds between layers in CLFD is much weaker than that in conventional FDM as the extrusion force from the nozzle tip is much smaller without sufficient contact with the top surface of filament.

Hence, it is very important to obtain sufficient lateral bonding in the fabrication process of a curved surface.

In the determination of the extruder path from sampling points on the curved surface, it should be noted that the distance between the nozzle tip and the depositing layer (the center of deposited filament's cross section) is expected to be adaptively changed based on the local geometric information of the surface. This distance is always set to be half of the layer thickness in flat FDM process, but in CLFD, the extruder path is not only affected by the spatial location of the points, but also dependent on their specific locations of the surface. As shown in Fig. 5a, the distance between the nozzle tip and depositing layer H in position P is

Fig. 4 Extrusion and deposition process of curved layer manufacturing. **a** Modeling of CLFD process. **b** Detail of the nozzle tip. **c** The shape of deposited filament. **d** the geometric detail of the filament

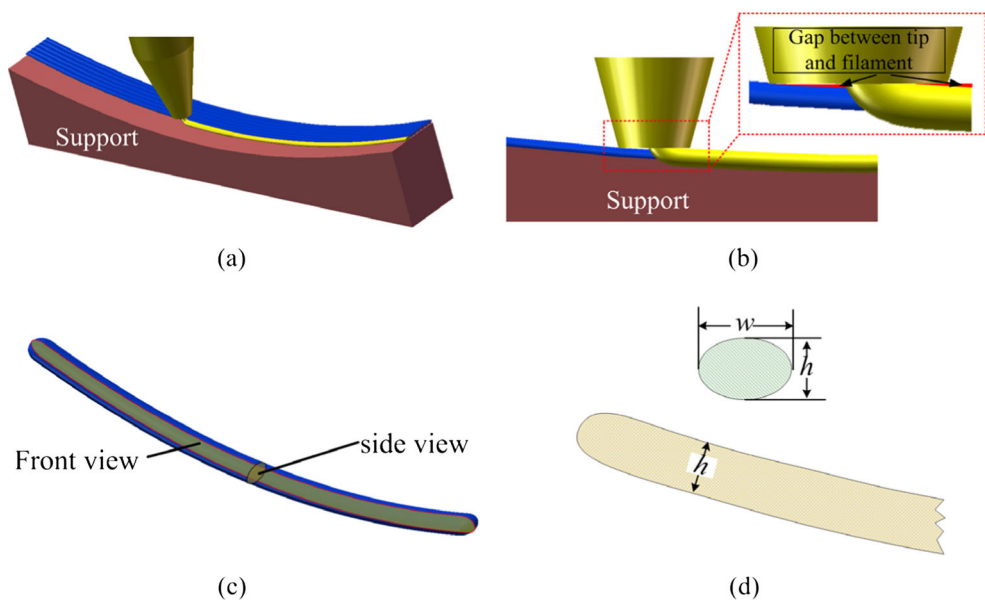
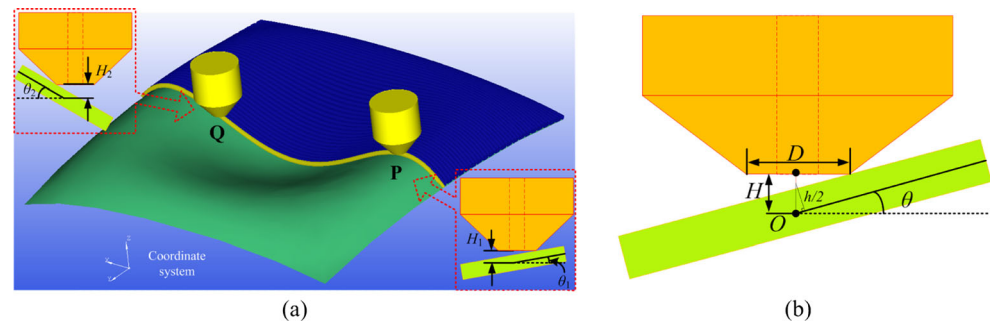


Fig. 5 Demonstration of the distance between the nozzle tip and the target location of the filament. **a** The distance between nozzle tip and depositing layer of different points on the surface. **b** Calculation of the distance



supposed to be smaller than that in position **Q** because the inclination angle in point **P** is smaller. In Fig. 5b, we assume that the target point is **O** and the inclination angle of filament path here is the tangent angle θ along the tangent of the deposition filament. As the curvature variation is very tiny within a small length long the path, we can adopt the inclination angle in point **O** for the computation. In case of the contact between the edge of the nozzle tip and former layers, the distance between the nozzle tip and the target filament location H should be larger than that in Eq. (1).

$$H = \frac{h/2}{\cos\theta} + \frac{D}{2}\tan\theta \quad (1)$$

where D is the outer diameter of the tip. Hence, we can get the relative location of the nozzle if the target position for the deposited filament has been specified. However, we need to notice that the distance obtained from Eq. (1) is a conservative value without any information on the filament deposition direction, which would impose an effect on the results. As shown in Fig. 6a–b, when the deposition direction is from right to left, the required distance is as calculated in Eq. (1), but if the deposition direction is the opposite, the resulted distance is smaller and calculated as Eq. (2).

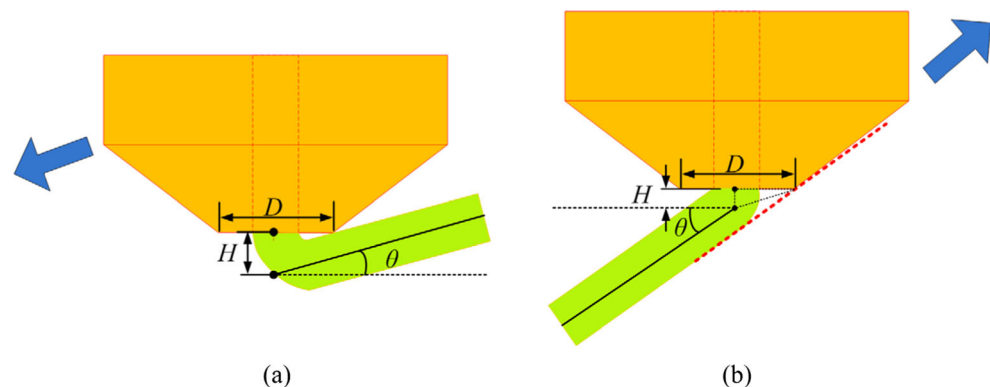
$$H = \frac{D}{4}\tan\theta. \quad (2)$$

Actually, besides the intervention along the direction tangent to the deposited filament, the direction normal to

the filament on the surface should be considered together. Likewise, different deposition directions bring in distinct distances between the nozzle tip and the target filament point. Specifically, if the higher side of the nozzle on the surface has been deposited, the distance should be calculated based on Eq. (1), while the distance should be obtained according to Eq. (2) when the depositing work is from the opposite direction. One point need to be noted is that the inclination angle is computed based on the vector that is normal to the tangent of the deposition filament. So, a distance H_1 is obtained based on the inclination angle θ_1 along the direction tangent to the deposited filament, another distance H_2 is computed based on the inclination angle θ_2 along the direction normal to the deposited filament, the final distance H between the nozzle tip and the filament target point is the larger one from these two values.

In our work, we define the target point for the filament deposition as filament target (FT) point, while the point of the extruder tip is defined as extruder location (EL) point. The FT point is the center of the cross section of the deposited filament and is obtained based on the shape of the reproduced surface similar to the CL (cutter location) points in traditional tool path generation for CNC milling. Thereafter, the EL points are generated based on the determined FT points and related geometric parameters for controlling the motion platform. So, the extruder path generation for CLFD can be accomplished by two sequential steps: planning the FT paths by considering the formed surface profile and generating EL paths.

Fig. 6 Illustration of the distance between the nozzle tip and the target location of the filament with different moving directions. **a** Moving from higher to lower. **b** Moving from lower to higher



In the CLFD, the surface of the top-most deposited layer is used to approximate and reconstruct the part surface, so the geometry of this layer from the slicing procedure should fully represent the surface. Based on this requirement, the slicing in the CLFD can be described as follows: the first layer is generated based on the geometric characterization of the part surface by surface fitting; then, the slicing surfaces are obtained by offsetting the surface. To ensure the distance between slicing surfaces is maintained at the constant layer thickness, the points on the original surface should be offset along its normal direction. These offset slicing surfaces are utilized to intersect with the fabricated part and the boundaries for the following extruder path generation are obtained.

3 Process planning for CLFD

Slicing and path planning are two critical tasks in the process planning and both play significant roles in the fabrication process and performance of the final fabricated parts. So this section will propose some algorithms and strategies for these two important aspects in CLFD.

3.1 Slicing procedure

The B-spline surface is used in this study to model the curved surface to be fabricated as it has been broadly used in the path planning, from which some approaches and methods can be referred. The diffused exchange file in the additive manufacturing is STL, which is a tessellated file format using numerous triangles to approximate the original part. So, the first step is to fit the mesh surface with a B-spline surface through all the fitting points chosen based on some criteria. A B-spline surface can be described as a tensor product defined by a topologically rectangular set of control points and two knot vectors associated with two independent parameters u and v , and it can be given by [29]

$$\mathbf{S}(u, v) = \sum_{i=0}^k \sum_{j=0}^l \mathbf{p}_{i,j} R_{i,j}(u, v) \quad (3)$$

with

$$R_{i,j}(u, v) = \frac{N_{i,n}(u)N_{j,m}(v)\omega_{i,j}}{\sum_{p=1}^k \sum_{q=1}^l N_{p,n}(u)N_{q,m}(v)\omega_{p,q}} \quad (4)$$

as rational basis functions, where $N_{i,n}(u)$ and $N_{j,m}(v)$ are the B-spline basis functions in the biparametric u and v , n and m are the order of two parameters, $\mathbf{p}_{i,j}$ represents the control points, $k+1$ and $l+1$ are the number of the control points in u and v

parametric directions, respectively. $\omega_{i,j}$ is the weight of the control points $\mathbf{p}_{i,j}$.

The fitting points on the surface are chosen from the vertices of triangles of STL file. As the number of vertices is pretty large when the STL model has a relatively high precision to preserve tiny features, it is absolutely unnecessary to add all the vertices into the set of fitting points. It can be accomplished by the reduction of the number of triangles with an acceptable error tolerance. It should be noted that the number of triangles would directly affect the surface accuracy, so the triangle representing some critical features cannot be missed. After the number of vertices and the precision requirement have both reached controllable and acceptable range, all the vertices on the surface are picked up and adopted to fit into a B-spline surface.

This fitted B-spline surface is named as reference slicing surface (RSS), which is used for the generation of slicing surfaces by the process of normal offsetting. In obtaining offset surface based on the RSS, there are two optional approaches: the first method is offsetting the RSS along the normal vectors directly by a distance of the layer thickness; another approach is generating the offset surface by offsetting the triangles that are used for the fitting process of RSS. The former method contains three steps: pick up points on the RSS, offset these points along its normal direction by a distance of layer thickness, and fit all the offset points into a new surface and this new surface can be expressed by the following:

$$\mathbf{S}'(u, v) = \mathbf{S}^0(u, v) + n^*t \cdot \mathbf{n}(u, v) \quad (5)$$

where $\mathbf{S}'(u, v)$ is the new slicing surface, $\mathbf{S}^0(u, v)$ is the RSS, t is the slice thickness, n^*t is the offset distance of n th. $\mathbf{n}(u, v)$ is the unit normal vector of one point $\mathbf{p}(u, v)$ on the surface as given by the following:

$$\mathbf{n}(u, v) = \frac{\mathbf{S}_u \times \mathbf{S}_v}{|\mathbf{S}_u \times \mathbf{S}_v|} \quad (6)$$

where \mathbf{S}_u and \mathbf{S}_v are the partial derivatives of surface $\mathbf{S}(u, v)$ with respect to u and v , respectively. This process is illustrated in Fig. 7. The other strategy is more straightforward, the key is to address the self-intersection issue in triangular mesh offsetting. Then, the vertices on these triangles are adopted to fit into a new slicing surface.

Subsequently, the boundaries on each layer defined by the combination of sequential slicing surfaces and part surface are used for the generation of the extruder path. The current practice for achieving the boundaries is using a low efficient search algorithm to obtain points on the model surface, but more accurate and efficient algorithms will be studied in our ongoing work.

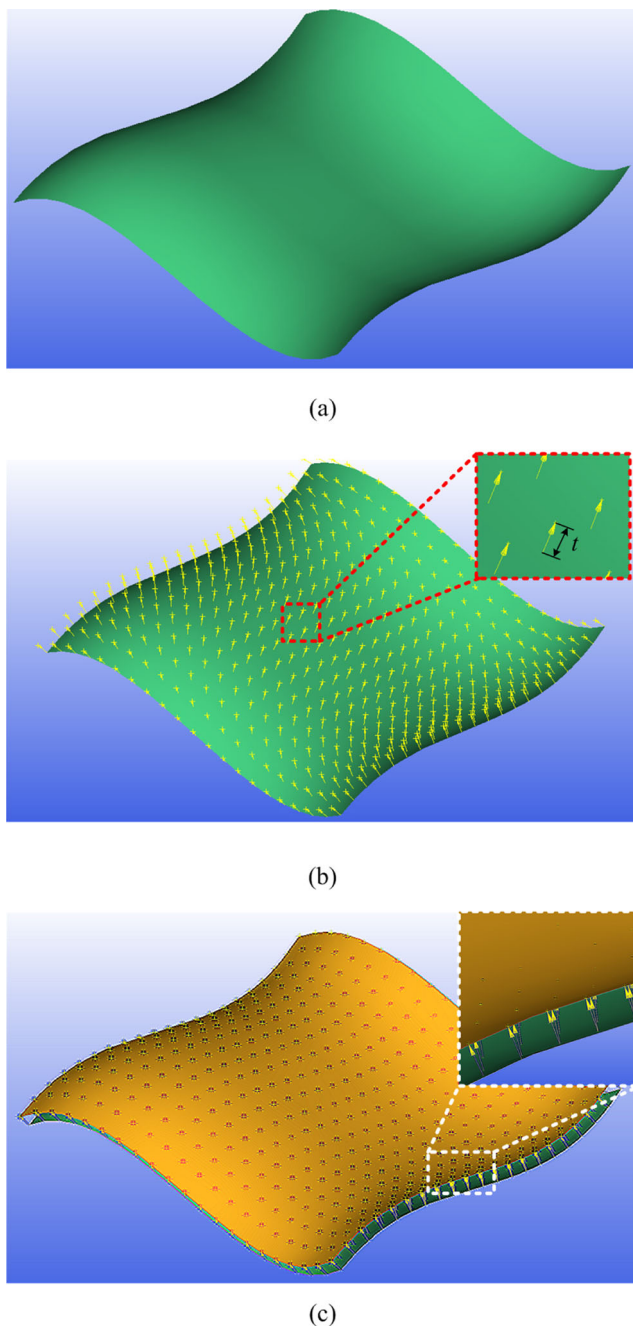


Fig. 7 Normal offsetting of a B-spline surface. **a** Reference slicing surface (RSS). **b** Generation of offsetting point sets. **c** Surface fitting based on point sets

3.2 Extruder path generation

As the top surface of fabricated parts is formed by the envelope of deposited filaments, the generation of FT points should consider the formed surface profile in terms of avoiding large voids between laterally adjacent filaments. It can be learned from the traditional tool path generation to acquire the filament paths on the basis of restricting the voids (scallop-height in traditional tool path generation) into a certain range. As shown in Fig. 8, the

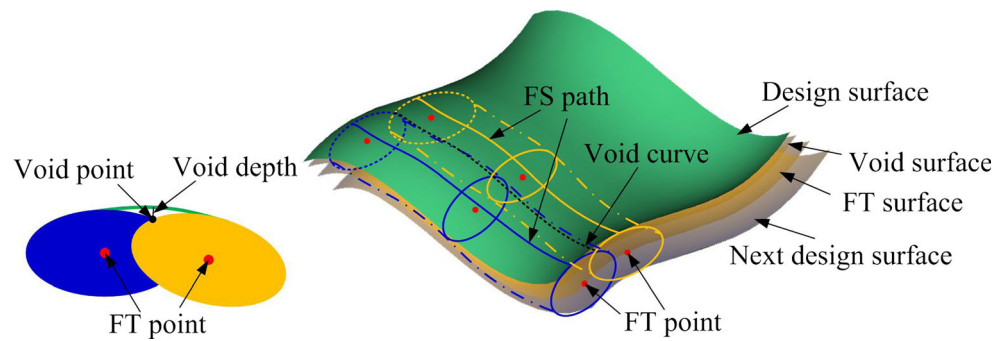
enveloping surface of the deposited filaments can be reckoned as the design surface. Here, the top curves of the filament on the surface are named as filament surface (FS) path which is similar to the definition of CC (cutter contact) path in traditional tool path planning with respect to the function of the part surface formation. And the lateral distance between adjacent filaments is referred to as the path interval, which is commonly known as the superposition (or overlap) of filaments resulting in the voids near the transient area, so the determination of FT paths should consider this phenomenon. The resulted voids between filaments affect the surface accuracy with an important parameter: void depth, which is defined as the distance between the bottom of the void and the design surface. All the bottoms tracing one path are called as a void curve. As for a fabricated surface with constant void depth, the bottom of all the voids is supposed to be located on an offset surface of the design surface with the void depth as the offset distance; this surface is named as void surface. This mentioned geometric information can be used in the determination of FT path with a given void depth.

In the present work, the extruder paths are obtained by following two steps. First, a surface is obtained by offsetting the design surface with an offset distance as half of layer thickness and this surface is called as FT surface; then, FT paths are generated based on a given FT path and the void depth requirement. Next, the established FT paths are used to build the EL paths according to Eqs. (1) and (2). In these two steps, the former is more important and difficult involving the determination of a void curve based on a given FS path and the next FS path is subsequently obtained, similar to those proposed by Feng et al. [30] for three-axis surface machining.

Figure 9 shows two laterally adjacent FT paths along which two filaments are going to be deposited. The void curve is the intersecting curve of two filaments and is on the void surface which is achieved by an offset of the design surface. For a point V_1 on the void curve, it is on the intersecting curve between a plane perpendicular to the tangent of a specified point F_1 on the FT path and the void surface. Combining the cross-sectional shape of the deposited filament, the point V_1 is determined. With the obtainable void point, the corresponding FT point on the next FT path is calculated by drawing a circle with the radius being the distance between points F_1 and V_1 in the plane that is perpendicular to the tangent of the void curve through the point V_1 and the intersection between this circle and the FT surface is the FT point. After all the FT points from a given FT path are generated, a new FT path is established.

Actually, the above method to generate the adjacent FS path originates from the typical tool path generation for CNC milling and the related algorithms can be found in [30]. However, the fundamental difference between

Fig. 8 Demonstration of some geometric relationship in extruder path generation



additive manufacturing and subtractive manufacturing has been figured out and handled in our work. The oval-shaped cross section of the deposited filament is used for determining the FT path and the void between lateral adjacent filaments is considered to ensure that the surface error is restricted.

After the generation of FT paths layer by layer, the corresponding EL paths are obtained based on Eqs. (1) and (2). These obtainable paths are then transferred to G code, which is able to control the movement of the nozzle to accomplish the fabrication process of curved surfaces.

4 Implementation and discussions

A bowl-like parametric surface is adopted in our study to verify the proposed methods and strategies for CLFD. The research in this paper is exploratory and requires further investigation in the practical application; we employ C++ language to realize all the proposed algorithms, and the results and details of the implementation are discussed as follows.

4.1 Slicing procedure

In the slicing procedure, the original tessellated surface is modified by reducing the number of triangles within a certain error tolerance, and then, the modified tessellated surface is fitted into a B-spline surface with two independent parameters u and v as the reference slicing surface (RSS) at first. The next

step is offsetting the original surface to obtain the remaining slicing surfaces according to the required layer thickness. Figure 10 shows the slicing surfaces generated with the surface-based offsetting method. In the offsetting process, the edge might be offset inwards when its normal vectors are in the incoming direction. Under this circumstance, the boundary of the offset surface might not have the intersection with the object, so there should be an enlargement coefficient for the offsetting. With all the obtainable offset slicing surfaces, the contours for each layer can be generated by calculating the intersecting curves between slicing surfaces and the part model.

Actually, the slicing procedure in our current work is the generation of many curved surfaces with a top-down direction to finally assist in the formation of the design top surface. So, the slicing procedure here contains three steps: (1) generation of slicing surfaces based on the RSS, (2) generation of a column from the edge of the RSS vertically, and (3) determination of the intersecting contour between the slicing surfaces and the column to obtain the sliced surface of each layer. This procedure evidently lacks the universality in practical fabrication for arbitrary models, so more applicable and universal slicing methods are required to be proposed for the diffusion of CLFD.

4.2 Extruder path planning

As for the extruder path planning, several steps are required.

- Step 1: All the obtained sliced surfaces are offset by a distance of the half of the layer thickness to get the FT surfaces.
- Step 2: The void surface is built by offsetting the design surface with a distance of the void depth based on the accuracy requirement.
- Step 3: The first FT path is chosen on the design surface along one of its edges; next, the corresponding void curve and the next FT path are calculated.
- Step 4: The extruder paths are generated based on the FT paths by offsetting the FT points vertically.

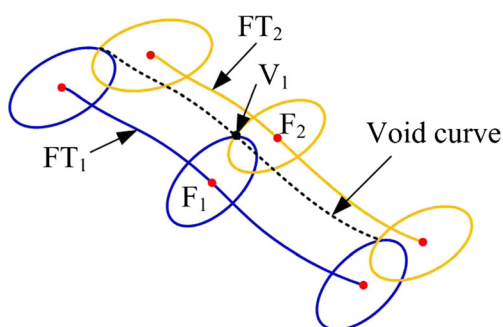


Fig. 9 Generation of the next FT path

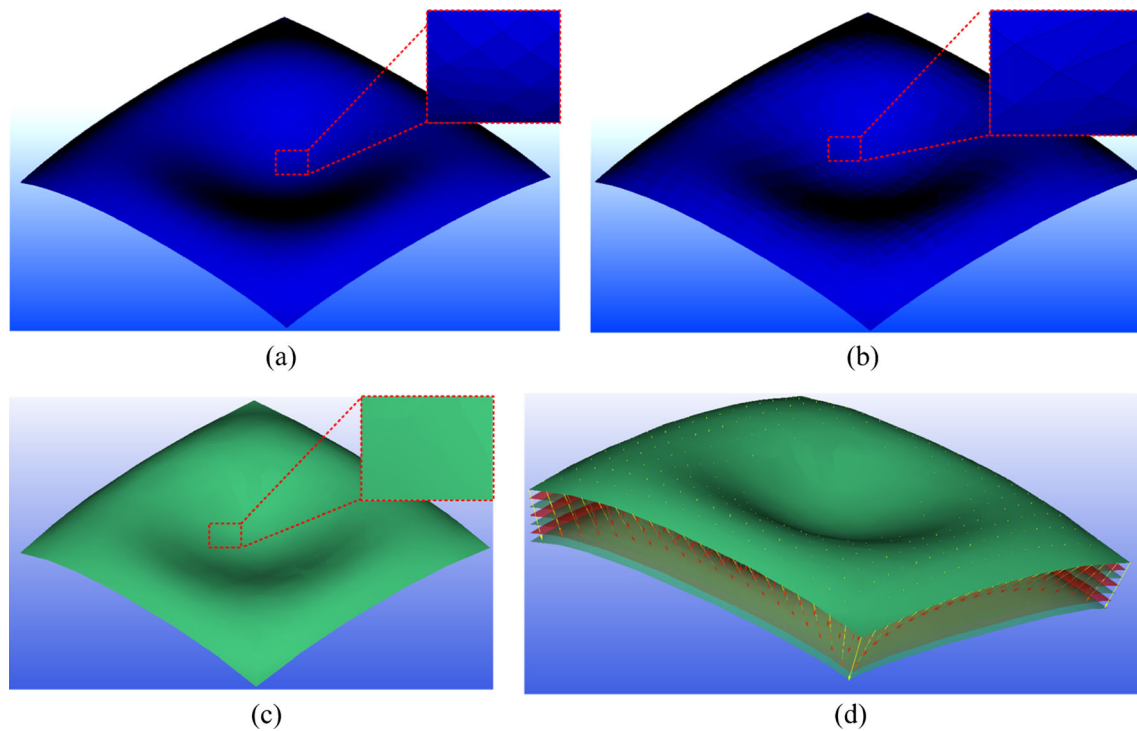


Fig. 10 Slicing process for the CLFD. **a** original STL file. **b** Modified STL file with less triangles. **c** Fitted B-spline surface. **d** Surface offset to obtain slicing surface

The first two steps are easy to realize with the same approaches as the aforementioned offsetting algorithm. In step 3, the initial FT path can be chosen arbitrarily on the FT surface in theory, but one of the edges of the surface is more preferable for the computational convenience. With considering this selected curve as the first FT path, the corresponding void curve and the next FT path can be determined by the following process and as demonstrated in Fig. 9.

As the cross sections of the filament at specific points on FT path F_1 is normal to the tangents of FT path, the corresponding void point V_1 must be on the intersecting curve between the plane normal to the tangent of the FT path at this specific point and the void surface. After that, the void point is obtained by considering the cross-sectional shape of the deposited filament. Based on this method, all the void points are generated and the void curve is fitted from these obtainable void points into a spline curve.

With a specified point of the void curve V_1 , the determination of the corresponding point on the next FT path F_2 can be described as a geometric problem to find a point on the FT surface that has a same distance to the point V_1 as the distance between V_1 and F_1 . The points satisfying this condition have a large amount but majority of them should be eliminated. Here, we select the point on the plane that is perpendicular to the tangent of the void curve on V_1 that is the target FT point. So a circle with the center F_1 and radius $|V_1 - F_1|$ is drawn on the plane that is normal to the tangent of the void curve on V_1 and the intersecting point of this circle and the FT surface is the corresponding FT point F_2 .

Based on the above method, Fig. 11 shows the generated FT paths for the surface and the deposited results are constructed with the filaments with oval-like cross section.

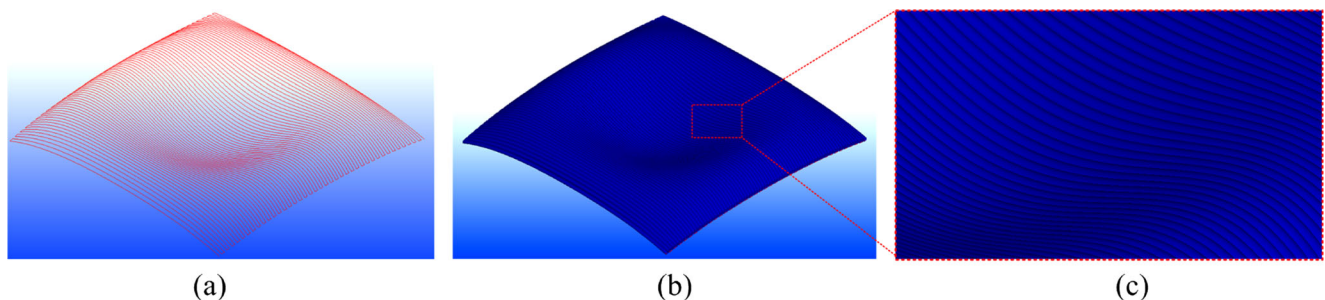


Fig. 11 Demonstration of the FT path generation. **a** FT paths. **b** Deposition results with oval-like filaments. **c** Detail of (b)

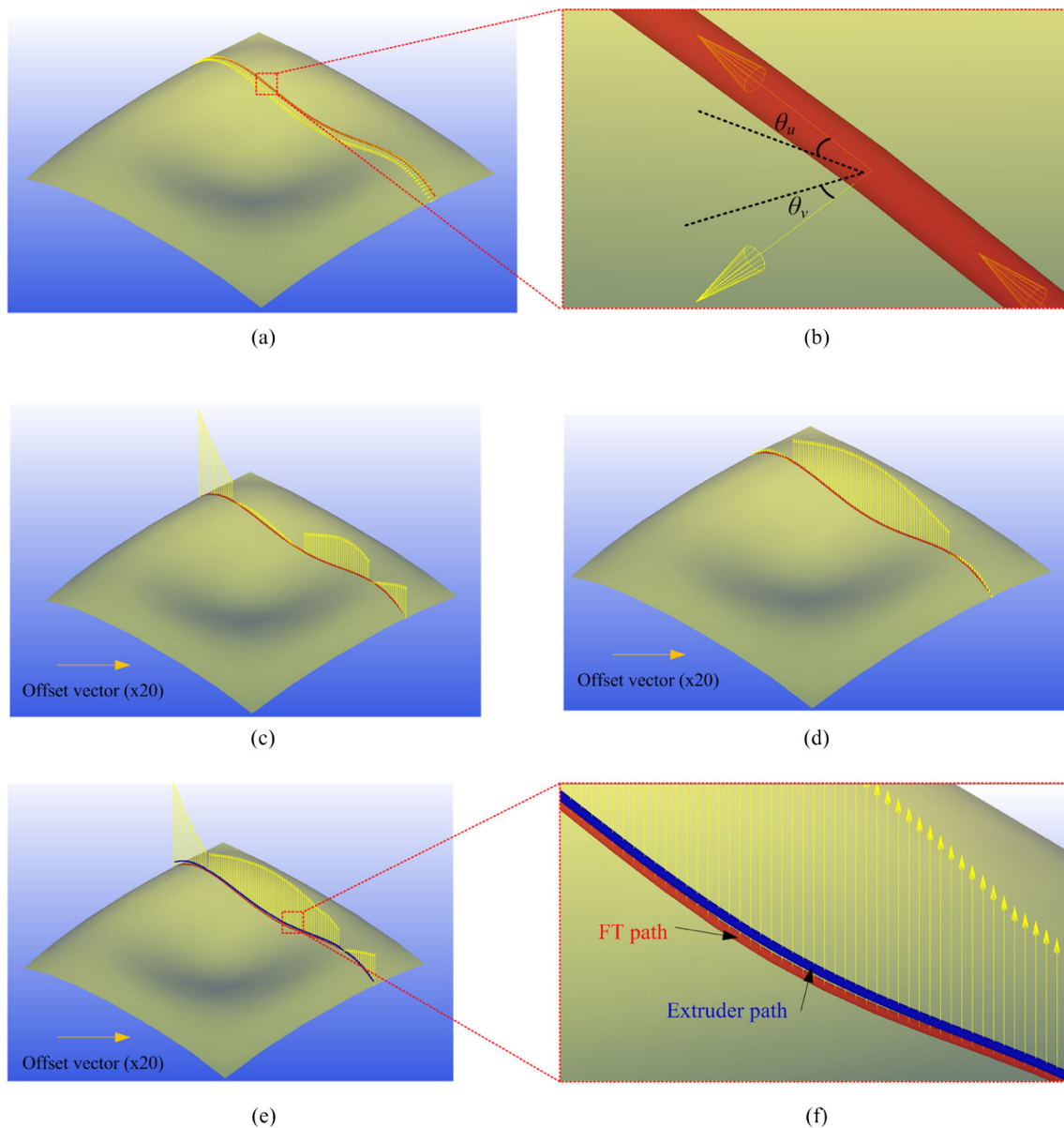


Fig. 12 Determination of extruder path based on the FT path. **a** Points on the FT path and their tangent vectors along two directions. **b** Detail of (a) and the inclination angles along two directions. **c** Offset distance based on

the tangent vector along u . **d** Offset distance based on the tangent vector along v . **e** Offset distance based on the larger value in (c) and (d). **f** Detail of (e)

The obtained FT paths need some subsequent modifications to get the final extruder path to control the extruder. As shown in Fig. 12, the FT points are adjusted based on the inclination angle of the point on the surface. The inclination angle is approximated with the angle between the tangent line and horizontal plane. The extruder path point is supposed to be higher vertically by a distance according to Eqs. (1) and (2) based on the corresponding point on the FT path. As illustrated in Fig. 12, the tangent vectors of points on FT path along two directions are calculated and the corresponding inclination angles are obtained. Based on these two angles θ_u and θ_v , the corresponding offsetting distances H_u and H_v are achieved as shown in Fig. 12c and d (the height in figures is magnified

20 times for easy visualization) with the height of the filament cross section that is 0.3 mm, and the diameter of the nozzle tip is 1.0 mm. Then, the larger distance along two directions at one certain point is selected as the final offset distance. The extruder path is generated finally based on the offset points in Fig. 12e and f.

Besides, the deposition of the filaments between layers should be accomplished in alternate directions just as done in general flat FDM. By doing this, the mechanical strength between successive layers would be much better by enhancing the isotropy in mechanical property.

Based on the demonstration and implementation of the proposed strategies and algorithms for the process planning

of CLFD, the major features and contributions of this research are as follows:

1. This work established the model of CLFD by fully considering the difference from the general flat FDM to figure out the key factors affecting the deposition process. Previous studies did not analyze the CLFD comprehensively and the reasons and details behind the differences were not provided. With the established model, the technical properties of CLFD could be identified which is conducive to improving the process planning.
2. The feasibility of CLFD with 3-axis machine was verified theoretically in our work via analyzing the orientation and location of the extruder along the path on the curved surface. Meanwhile, the limitation of the CLFD using 3-axis platform in terms of the curvature variation was confirmed from the analysis that was very helpful in the application of CLFD.
3. The cross-sectional shape of the deposited filament in CLFD was identified as oval based on the established model. The subsequent process planning of CLFD, especially in the path planning, was supposed to be accomplished with the identified shape. However, studies in this aspect had not been done in previous studies. Our work tried to fill this gap.
4. The computation of the distance between the nozzle tip and the underlying layer was formulated. To achieve desirable deposited curved surface, the factors influencing the distance between the nozzle tip and the underlying layer were analyzed. The relationship between the distance and the moving direction of the nozzle was built to distinguish different deposition directions. In addition, two inclination angles, one was along the direction tangent to the deposited filament, another was along the direction normal to the deposited filament, were both computed and compared for the determination of the final distance.
5. The slicing procedure of CLFD was demonstrated in our work and corresponding algorithms were proposed. Compared to existing methods for slicing, our method could preserve tiny features of the surface by sampling enough points near these features and the B-spline surface was adopted to represent the curved surface for accurate and simple computation for the offsetting process.
6. The path planning method based on the above analyses was presented and different from those in previous studies in terms of the cross-sectional shape of deposited filaments, which was critical in affecting the bonding effect between lateral adjacent filaments. Meanwhile, the provided details of the proposed algorithms could be easily extended and applied to other AM techniques integrating some revisions.

5 Conclusions

In this paper, the modeling and process planning for curved layer fused deposition (CLFD) have been studied, as well as some critical strategies and algorithms in the process planning have been presented by fully considering the established model of CLFD. Before building the model of CLFD, the general fused deposition process was studied on the basis of the drum-like deposited filament. After that, the CLFD process was modeled and discussed in detail from several perspectives. Specifically, the orientation of the nozzle was discussed at first, and we found that it was not necessarily to be vertical when depositing the curved surface with an acceptable inclination; the difference in the cross-sectional shape between flat FDM and CLFD was analyzed for the subsequent steps; the distance between the nozzle tip and the former layer was formulated under two different circumstances and along two directions, respectively, for the determination of the extruder path. Based on these analyses, two important steps in the process planning were formulated and discussed. Related algorithms in the slicing procedure and extruder path planning have been proposed for the implementation of CLFD. At last, the proposed algorithms were applied in a bowl-like curved surface to verify the models and the algorithms. In summary, the works in this research provided a systematical scheme of the CLFD and some key issues of this potential technique have been pointed out that is really beneficial for the development of AM technology.

Although the CLFD exhibits wide fabrication capability in many potential applications, some limitations in both the computer-aided-design (CAD) and computer-aided-manufacturing (CAM) stages, such as the processing of part surface, support generation for the curved parts need to be solved based on the process characteristics of CLFD. So, further investigations and studies will be required in these aspects to incorporate the CLFD in the current additive manufacturing techniques to extend their flexibility and functionality.

Acknowledgments This paper is sponsored by the National Natural Science Foundation of China (No. 51375440), and also sponsored by K.C. Wong Magna Fund in Ningbo University and Scientific Research Starting Foundation of Ningbo University (No. 421610040).

References

1. Wong KV, Hernandez A (2012) A review of additive manufacturing. *ISRN Mech Eng* 2012:1–10. doi:10.5402/2012/208760
2. Steuben JC, Iliopoulos AP, Michopoulos JG (2016) Implicit slicing for functionally tailored additive manufacturing. *Comput Des* 77: 107–119. doi:10.1016/j.cad.2016.04.003
3. Pandey PM, Reddy NV, Dhande SG (2003) Improvement of surface finish by staircase machining in fused deposition modeling. *J Mater Process Technol* 132:323–331

4. Wang J, Xie H, Weng Z et al (2016) A novel approach to improve mechanical properties of parts fabricated by fused deposition modeling. *Mater Des* 105:152–159. doi:[10.1016/j.matdes.2016.05.078](https://doi.org/10.1016/j.matdes.2016.05.078)
5. Boschetto A, Bottini L (2016) Design for manufacturing of surfaces to improve accuracy in fused deposition modeling. *Robot Comput Integr Manuf* 37:103–114. doi:[10.1016/j.rcim.2015.07.005](https://doi.org/10.1016/j.rcim.2015.07.005)
6. Liu X, Shapiro V (2016) Homogenization of material properties in additively manufactured structures. *Comput Des* 78:71–82. doi:[10.1016/j.cad.2016.05.017](https://doi.org/10.1016/j.cad.2016.05.017)
7. Boschetto A, Bottini L (2014) Accuracy prediction in fused deposition modeling. *Int J Adv Manuf Technol* 73:913–928. doi:[10.1007/s00170-014-5886-4](https://doi.org/10.1007/s00170-014-5886-4)
8. Ahn D, Kweon JH, Kwon S et al (2009) Representation of surface roughness in fused deposition modeling. *J Mater Process Technol* 209:5593–5600. doi:[10.1016/j.jmatprotec.2009.05.016](https://doi.org/10.1016/j.jmatprotec.2009.05.016)
9. Boschetto A, Giordano V, Veniali F (2012) Modelling micro geometrical profiles in fused deposition process. *Int J Adv Manuf Technol* 61:945–956. doi:[10.1007/s00170-011-3744-1](https://doi.org/10.1007/s00170-011-3744-1)
10. Jin Y, Li H, He Y, Fu J (2015) Quantitative analysis of surface profile in fused deposition modeling. *Addit Manuf* 8:142–148. doi:[10.1016/j.addma.2015.10.001](https://doi.org/10.1016/j.addma.2015.10.001)
11. Boschetto A, Bottini L, Veniali F (2016) Finishing of fused deposition modeling parts by CNC machining. *Robot Comput Integr Manuf* 41:92–101. doi:[10.1016/j.rcim.2016.03.004](https://doi.org/10.1016/j.rcim.2016.03.004)
12. Rahmati S, Vahabli E (2015) Evaluation of analytical modeling for improvement of surface roughness of FDM test part using measurement results. *Int J Adv Manuf Technol* 79: 823–829. doi:[10.1007/s00170-015-6879-7](https://doi.org/10.1007/s00170-015-6879-7)
13. Sood AK, Ohdar RK, Mahapatra SS (2009) Improving dimensional accuracy of fused deposition modelling processed part using grey Taguchi method. *Mater Des* 30:4243–4252. doi:[10.1016/j.matdes.2009.04.030](https://doi.org/10.1016/j.matdes.2009.04.030)
14. Bansal R (2011) Improving dimensional accuracy of fused deposition modelling (FDM) parts using response surface methodology. *Proc Inst Mech Eng Part E J Process Mech Eng* 219:89–92. doi:[10.1243/095440805x6964](https://doi.org/10.1243/095440805x6964)
15. Pennington RC, Hoekstra NL, Newcomer JL (2005) Significant factors in the dimensional accuracy of fused deposition modelling. *Proc Inst Mech Eng Part E J Process Mech Eng* 219:89–92. doi:[10.1243/095440805x6964](https://doi.org/10.1243/095440805x6964)
16. McCullough EJ, Yadavalli VK (2013) Surface modification of fused deposition modeling ABS to enable rapid prototyping of biomedical microdevices. *J Mater Process Technol* 213:947–954. doi:[10.1016/j.jmatprotec.2012.12.015](https://doi.org/10.1016/j.jmatprotec.2012.12.015)
17. Galantucci LM, Lavecchia F, Percoco G (2010) Quantitative analysis of a chemical treatment to reduce roughness of parts fabricated using fused deposition modeling. *CIRP Ann - Manuf Technol* 59:247–250
18. Chakraborty D, Aneesh Reddy B, Roy Choudhury A (2008) Extruder path generation for curved layer fused deposition modeling. *CAD Comput Aided Des* 40:235–243. doi:[10.1016/j.cad.2007.10.014](https://doi.org/10.1016/j.cad.2007.10.014)
19. Patel Y, Kshattriya A, Singamneni SB, Roy Choudhury A (2015) Application of curved layer manufacturing for preservation of randomly located minute critical surface features in rapid prototyping. *Rapid Prototyp J* 21:725–734. doi:[10.1108/RPJ-07-2013-0073](https://doi.org/10.1108/RPJ-07-2013-0073)
20. Singamneni S, Diegel O, Huang B (2010) Curved layer fused deposition modeling. *Aut Univ*
21. Huang B, Singamneni S, Diegel O (2008) Construction of a curved layer rapid prototyping system: integrating mechanical, electronic and software engineering. *Int. Conf. Mechatronics Mach. Vis. Pract, In*, pp. 599–603
22. Singamneni S, Roychoudhury A, Diegel O, Huang B (2012) Modeling and evaluation of curved layer fused deposition. *J Mater Process Technol* 212:27–35
23. Huang B, Singamneni S (2012) Alternate slicing and deposition strategies for fused deposition modelling of light curved parts. *J Achiev Mater Manuf Eng* 55
24. Huang B, Singamneni SB (2015) Curved layer adaptive slicing (CLAS) for fused deposition modelling. *Rapid Prototyp J* 21: 354–367
25. Huang B, Singamneni S (2013) Curved layer fused deposition modeling with varying raster orientations. *Appl Mech Mater* 446-447:263–269
26. Huang B, Singamneni S (2014) A mixed-layer approach combining both flat and curved layer slicing for fused deposition modelling. *Proc Inst Mech Eng Part B J Eng Manuf*:229
27. Allen RJA, Trask RS (2015) An experimental demonstration of effective curved layer fused filament fabrication utilising a parallel deposition robot. *Addit Manuf* 8:78–87
28. Turner BN, Strong R, SA G (2014) A review of melt extrusion additive manufacturing processes: I. Process design and modeling. *Rapid Prototyp J* 20:192–204. doi:[10.1108/RPJ-01-2013-0012](https://doi.org/10.1108/RPJ-01-2013-0012)
29. Piegl L, Tiller W (1987) Curve and surface constructions using rational B-splines. *Comput Des* 19:485–498
30. Feng HY, Li H (2002) Constant scallop-height tool path generation for three-axis sculptured surface machining. *Comput Des* 34:647–654